Supplementary Information (SI) for Chemical Communications.

Supporting information for

Metal-Free Carbon Catalysts for Highly Selective Electrocatalytic Reduction of Nitrostyrene

Shiqi Li, Wenbin Zhang, Songlin Liu, Min Hu, Yuchen Lei, Yun Zhang, Wei Zhao*

Institute for Advanced Study, Shenzhen University, Shenzhen, Guangdong 518060, China.

* Correspondence and requests for materials should be addressed to Wei Zhao (weizhao@szu.edu.cn)

Experimental Section

Chemicals and reagents

Nafion 117 membrane (Chemours), platinum mesh , ethanol (99.7%, Macklin), sulfuric acid (H_2SO_4, 98%, Sigma-Aldrich), potassium hydroxide (KOH, 95%, Macklin), sodium sulfate (Na_2SO_4, 99%, Aladdin), copper sulfate ($CuCl_2$, 99%, Macklin) palladium chloride ($PdCl_2$, Innochem), chloroplatinic acid (H_2PtCl_6, Aladdin), ruthenium chloride ($RuCl_3$, Aladdin)，Guaiacol (99%, Acros Organics), trichloromethane ($CHCl_3$, 99.8%, Aladdin), 3-nitrostyrene (98%, Innochem), 3-ethylaniline (97%, Innochem), 3-vinylaniline (98%, Innochem).

Catalysts synthesis

Preparation of oxidized graphite fibers (OGF)

The graphite fibers were sequentially washed with acetone, ethanol, and deionized water under ultrasonication and dried at 70°C for 10 hours. Then these fibers were subjected to anodic oxidation treatment within a three-electrode cell system. The oxidation was conducted at a constant current density of 90 mA cm^{-2} for 25 min in 0.2 M H_2SO_4 aqueous solution. Following the oxidation, the treated graphite fibers were washed with deionized water and dried at 80°C for 12 hours, and the resulting modified graphite fibers were designated as OGF. In this work, the OGF serves as the primary catalyst investigated.

Preparation of reduced graphite fibers (RGF)

For the reduction process, the graphite fibers were prepared following the same initial procedure. Then, the pre-treated graphite fibers were placed in a tube furnace. Initially, a mixture of H_2/Ar (5% H_2) was delivered into the furnace for 30 min to purge the air. Subsequently, the furnace was heated to 400°C under a hydrogen-argon atmosphere at a rate of 2°C/min, and the graphite fibers were roasted at this temperature for 2 hours. After this reduction treatment, these graphite fibers were labeled as RGF.

Ru/GF, Pt/GF and Pd/GF electrocatalysts preparation

We synthesized Ru/GF, Pt/GF and Pd/GF electrocatalysts by the wet-chemical method then by calcination. The graphite fibers were initially cleaned sequentially with ethanol and deionized water under ultrasonication. Aliquots (0.35 mL each) of 200 mM metal precursor solutions ($RuCl_3$, H_2PtCl_6, or $PdCl_2$) were separately prepared and drop-coated onto pretreated graphite fibers substrates through multiple deposition steps. Next, the impregnated graphite fibers were placed in the tube furnace. Before calcination, argon gas was introduced to purge the air from the furnace. Subsequently, under an argon atmosphere, the furnace temperature was raised to 500°C at a rate of 5°C/min, and the fibers were calcined for 2 hours. As a result, we obtained Ru/GF, Pt/GF, and Pd/GF materials that are ready for direct application as cathodes.

Cu/GF electrocatalyst preparation

In a typical procedure, the Cu/GF electrocatalyst was synthesized by electrodepositing copper onto the graphite fibers, within a three-electrode electrochemical cell. The Cu/GF catalyst was synthesized using the aqueous electrolyte containing 0.5 M Na_2SO_4 and 10 mM $CuCl_2$. And this electrodeposition involved 50 cyclic voltammetry cycles, scanning the potential from -1.5 to 1.7 V (vs. Ag/AgCl) at a scan rate of 0.1 $V\cdot s^{-1}$. After the electrodeposition, the working electrode was rinsed with deionized water and dried at ambient conditions. Carbon paper and an Ag/AgCl electrode were used as the counter electrode and reference electrode, respectively.

Materials characterization

Used scanning electron microscope (SEM, Thermo Scientific Apreo 2C) equipped with EDX detectors was used to characterize the OGF morphology. The functional groups present in the OGF were analyzed by Fourier transform infrared spectroscopy (FT-IR, Thermo Scientific Nicolet iS50) using the KBr pellet method (4000–400 cm^{-1}). Additionally, the surface functional groups of OGF were analyzed by X-ray photoelectron spectroscopy (XPS, PHI GENESIS 500) under an ultra-high vacuum pressure of 10^{-7} Pa. The specific surface area was determined by N_2 adsorption measurements using a surface area and porosity analyzer (CIQTEK Climber 60). The corresponding N_2 adsorption isotherm was presented in Figure S18.

Electrochemical measurements

The electrocatalytic reduction of 3-NS to 3-VA was performed in an airtight two-compartment electrochemical cell separated by a bipolar membrane (HMBM-4012) with a magnetic stirring at 500 rmp. The catholyte was a 20 mL EtOH/H_2O mixture (volume ratio of 3: 2) containing 0.16 M H_2SO_4 and 10 mM 3-NS, with ethanol was added to improve the dispersion of 3-NS. And the anolyte consisted of 1 M KOH. Electrochemical measurements were conducted with a triple-electrode system: the OGF or M/GF (M=Cu, Pd, Pt and Ru) catalysts were used as the working electrodes with an area of 1*1 cm^2 exposed to the electrolyte in each run of the electrochemical test, an Ag/AgCl (R0302, Tianjin Aida Hengsheng) electrode was used as the reference electrode and a Pt mesh was used as the counter electrode. Before the electrochemical tests, the M/GF (M = Cu, Pd, Pt, and Ru) catalysts underwent a reduction treatment: specifically, a potential of -1 V (Vs. Ag/AgCl) was applied in 0.1 M Na_2SO_4 solution for 30 minutes. All electrochemical tests were performed on the electrochemical workstation (CHI 760E) under ambient conditions.

ECH product analysis

The liquid products were collected at one hour as indicated in the main text. The quantification of the liquid products was performed utilizing the gas chromatography mass spectrometry system (GC-MS 7890B-5977A, Agilent), which was equipped with a HP-5 ms column (30 m * 0.25 mm * 0.25 µm, Agilent). The internal standard employed was guaiacol. The internal standard method was used for calibration and product standard curves were prepared for quantitative analysis of the experimental results.

Injector temperature was set to 250°C with a split ratio of 30:1. At the beginning, the oven program was heated from 90°C to 200°C in 8 min, then maintained at 200°C for 1.5 min, then it took 3.5 min to heat from 200°C to 280°C and maintained at 280°C for 0.5 min, finally, increase from 280°C to 310°C in 1.75 min.

Prior to the product analysis, the reaction solution needs to be extracted, the extractant is trichloromethane (CCl_3), the volume ratio of CCl_3 to the reaction solution is 1: 1 for extraction, and then the organic phase was analysed. The conversion of the reactants, the selectivity of the products, the FE (%) of the products and the productivity of products were calculated according to the following equations:

Conversion of 3-NS:

$$Conversion = \frac{n_{3-NS,0} - n_{3-NS,rest}}{n_{3-NS,0}} \times 100\%$$

Selectivity of products:

$$Selectivity = \frac{n_i}{n_{3-NS,0} - n_{3-NS,rest}} \times 100\%$$

Faradaic efficiency of products:

$$FE = \frac{n_i Z_i F}{Q_{pass}} \times 100\%$$

Productivity of products:

$$Productivity = \frac{n_i}{area\ of\ WE * t}$$

where $n_{3\text{-}NS,0}$ and $n_{3\text{-}NS,rest}$ are the initial and final numbers of moles of 3-NS; n_i is the number of moles of product *i*; Z_i is the number of electrons transferred for the corresponding reduction process from 3-NS to product i ,Z was 2 for 1-nitroso-3-vinylbenzene (NV), 2 for 3-nitroethylbenzene (3-ENB), 6 for 3-vinylaniline (3-VA) and 8 for 3-ethylaniline (3-EA); *F* is the faradaic constant (*F*= 96,485 C mol^{-1}); Q_{pass} is the total charge transferred in the system ($Q_{pass} = I \times t$). Here, area of WE in the productivity formula represents the geometrical area of working electrode as 1 cm^2. Unless otherwise stated, all potential data have been converted into reversible hydrogen electrode equation as follows:

$$E(V\ vs.RHE) = E(V\ vs.\ Ag/AgCl) + 0.059 \times pH + 0.197$$

Adsorption energy calculation

First-principles calculations were performed using the CASTEP package within the framework of density functional theory (DFT). The exchange–correlation interactions were described by the Perdew–Burke–Ernzerhof (PBE) functional under the generalized gradient approximation (GGA). A plane-wave cutoff energy of 550 eV and Monkhorst–Pack k-point meshes with a reciprocal-space spacing of 0.04 $Å^{-1}$ were adopted to ensure energy convergence. All structures were fully relaxed until the residual atomic forces were below 0.03 eV $Å^{-1}$ and the total energy variation was less than 1×10^{-6} eV $atom^{-1}$. A vacuum layer larger than 20 Å was applied to eliminate spurious interactions between periodic images. The adsorption energy was evaluated as $E_{ads}=E_{surface+adsorbate}-E_{surface}-E_{adsorbate}$. Charge redistribution upon adsorption was analyzed through charge-density-difference mapping, defined as $\rho_{ads}=\rho_{surface+adsorbate}-\rho_{surface}-\rho_{adsorbate}$.

Table S1. Comparison for the electrocatalytic reduction of nitrostyrene with different reaction conditions reported in the previous literature. Data with a symbol “*” means that it was recalculated from the corresponding paper. The calculated current densities are the average current densities. The calculation process is as below

Catalysts	**Reactant**	**J mA/cm^2**	**FE (%)**	**Generation rate mmol/h/cm^2**	**Time（h）**	**Ref**
OGF	3-NS	30	79	0.146	1	This work
Mo_2C@MoS_2	4-NS	6.5*	85	0.03517	5	report[1]
Pd-Mo metallene	4-NS	6*	84	0.0588	5	report[2]
Co_3S_{4-x}NS	4-NS	-	86	0.07	6	report[3]
CoP	4-NS	-	-	0.07	6	report[4]
MoS_2-DMA	4-NS	4*	100	0.025*	5	report[5]
CNT	4-NS	-	-	$8.3*10^{-4}$*	4	report[6]

We used stable chronopotentiometric operation for electrocatalytic reduction of 3-NSRR. As the previously reported papers used stable chronoamperometric operation, their current densities changed with the reaction, and there was no constant value of current density, so the average current densities were used for comparison. Thus, the current densities calculated above are the average current densities, not the highest or lowest value. (The areas used in the relevant calculations in the table are all geometric areas)

Take Mo_2C@MoS_2 metallene for example. The equations used in the calculation are following.

$$Generation\,rate = \frac{n_{NS}}{5 \times 1.5\,cm \times 1.5\,cm} = 0.03517 mmol\,h^{-1} cm^{-2}$$

$$\text{So } n_{NS} = 0.03517 \times 5 \times 1.5 \times 1.5 = 0.39\,mmol$$

$$FE = \frac{6 \times 96485 \times 0.39 \div 1000}{Q} \times 100\% = 85\%$$

$$So\ Q = \frac{6 \times 96485 \times 0.39 \div 1000}{0.85} = 265C$$

$$So\ I_{avg} = \frac{265C}{5 \times 3600 \times 1.5cm \times 1.5cm} = 6.5\,mA\,cm^{-2}$$

Table S2. Comparison of ECSA-normalized current density and production rate for catalysts reported in the previous literature. Data with a symbol "*" means that it was recalculated from the corresponding paper, while date with a symbol "-" means that the ECSA value or FE value was not provided in the literature. The calculated current densities are the average current densities.

Catalysts	**Reactant**	**J mA/cm $_{ECSA}^2$**	**Generation rate mmol/h/cm$_{ECSA}^2$**	**Ref**
OGF	3-NS	3.1	0.015	This work
$Mo_2C@MoS_2$	4-NS	1.3*	0.007	report[1]
Pd-Mo metallene	4-NS	0.18*	$0.93*10^{-3}$	report[2]
$Co_3S_{4-x}NS$	4-NS	-	-	report[3]
CoP	4-NS	-	-	report[4]
MoS_2-DMA	4-NS	-	-	report[5]
CNT	4-NS	-	$0.49*10^{-5}*$	report[6]

Techno-economic analysis (TEA)

We performed a TEA to evaluate the technoeconomic feasibility of electrocatalytic reduction of 3-NS using a modified model (Table S1) of previous works.[7-10] The plant capacity was set at 1000 kg/day for the production of 3-VA from 3-NS. The overall electrolyzer cost was determined at \$920/m^2, with reference to a documented CO_2 reduction electrolyzer case.[11] The membrane price is \$27.99 per square meter, while 3-NS is priced at 1 \$/kg and 3-VA at 25 \$/kg (data sourced from Baidu B2B Hub). The price of renewable electricity was set at 0.07 \$/kWh. Based on the recently published literature, the cost associated with the separation process was defined as 20% of the total cost.

TEA cost components

We calculate the cost components using the following equations:

Total Current (A): The total current consumed by the electrolyzer system to achieve a production rate of 1000 kg per day.

$$Total\ current\ (A) = \frac{1000\left(\frac{kg}{day}\right)}{119 \times 10^{-3}\left(\frac{kg}{mol}\right)} \times \frac{day}{86400s} \times 6e^{-} \times 96485\left(\frac{C}{mol}\right) \times \frac{1}{FE\%}$$

Total Surface Area (m^2): The total surface area of electrolyzer needed by the electrolyzer system to achieve a production rate of 1000 kg per day.

$$Total\ Surface\ (m^2) = Total\ current\ (A) \times \frac{1}{Current\ density\left(\frac{A}{m^2}\right)}$$

Power Consumed (kW): The total power consumed by the electrolyzer system to achieve a production rate of 1000 kg per day.

$$Power\ consumed\ (kW) = Total\ current\ (A) \times operating\ voltage\ (V) \times \frac{W}{1000KW}$$

Total Electrolyzer Cost (\$): The total electrolyzer cost is calculated by multiplying the total surface area required (in square meter) by the cost square meter (\$/m^2).

$$Total\ electrolyzer\ cost = Total\ surface\ (m^2) \times price\ per\ m^2\left(\frac{\$}{m^2}\right)$$

Capital Recovery Factor: The capital recovery factor is calculated the discount rate and the electrolyzer's lifetime, accounting for the time value of money.

$$Captical\ Recovery\ Factor(CRF) = \frac{Discount\ rate \times (1 + Discount\ rate)^{lifetime}}{(1 + Discount\ rate)^{lifetime} - 1}$$

The total cost of the proposed process consisted of capital cost, installation cost, balance of Plant, input chemicals cost, electricity cost, operational cost and maintenance cost.

Capital Cost:

1. Capital cost/kg of product ($/kg): the capital cost/kg of product per kilogram is calculated by dividing the product of total electrolyzer cost and capital recovery factor by the product of capacity factor, daily production quantity, and electrolyzer lifetime. The anticipated service life of the electrolyzer was 1 year, and the working time per year was 365 days.

$$Capital\ cost\ per\ kg\ of\ product \left(\frac{\$}{kg}\right) = \frac{Total\ electrolyzer\ cost\ (\$) \times CRF}{Capitcity\ factor \times 1000 \left(\frac{kg}{day}\right) \times Electrolyzer\ lifetime\ (year) \times 365 \left(\frac{day}{year}\right)}$$

2. Catalyst cost per kilogram of product ($/kg): The catalyst cost per kilogram was calculated by dividing the total catalyst cost (based on the area-specific price and the total electrode area) by the total production over the catalyst's lifetime. The anticipated service life of the catalyst was 1 year, and the working time per year was 365 days.

$$Catalyst\ cost \left(\frac{\$}{kg}\right) = \frac{GF\ price \left(\frac{\$}{m^2}\right) \times total\ Surface\ area\ (m^2)}{catalyst\ lifetime\ (year) \times 365 \left(\frac{day}{year}\right) \times 1000 \left(\frac{kg}{day}\right)}$$

3. Membrane cost per kilogram of product ($/kg): The membrane cost per kilogram is calculated by dividing total membrane cost by the total production over the membrane's lifetime. The anticipated service life of the membrane was 1 year, and the working time per year was 365 days.

$$Membrane\ cost \left(\frac{\$}{kg}\right) = \frac{membrane\ price \left(\frac{\$}{m^2}\right) \times total\ Surface\ area\ (m^2)}{membrane\ \ lifetime\ (year) \times 365 \left(\frac{day}{year}\right) \times 1000 \left(\frac{kg}{day}\right)}$$

Installation cost per kilogram of product ($/kg):

$$Installation \left(\frac{\$}{kg}\right) = Lang\ factor\ (\%) \times (capital\ cost\ per\ kg\ of\ product\ +\ catalyst\ cost\ +\ membrane\ cost) \left(\frac{\$}{kg}\right)$$

Balance of Plant cost per kilogram of product ($/kg):

$$Balance\ of\ plant\left(\frac{\$}{kg}\right) = Balance\ of\ plant\ factor\ (\%) \times (capital\ cost\ per\ kg\ of\ product\ +\ catalyst\ cost\ +\ membrane\ cost)\left(\frac{\$}{kg}\right)$$

Electricity cost per kilogram of product ($/kg):

$$Electricity\ cost\left(\frac{\$}{kg}\right) = \frac{Power\ consumed\ (KW) \times 24\left(\frac{hour}{day}\right) \times 0.07\left(\frac{\$}{kwh}\right)}{1000\left(\frac{kg}{day}\right)}$$

Maintenance cost per day ($/day):

$$Maintenance\ cost\left(\frac{\$}{day}\right) = Maintenance\ frequency\left(\frac{1}{day}\right) \times Maintenance\ factor\ (\%) \times capital\ cost\left(\frac{\$}{kg}\right)$$

Table S3. Model of techno-economic analysis (TEA) for electrocatalytic reduction of 3-NS. Modified model from the previous works.

Breakdown of TEA Details	
Capital cost	Capital cost per kg of product + catalyst cost + membrane cost + electrolyte cost
Installation cost	Lang factor (50%) × (capital cost per kg of product + catalyst cost + membrane cost)
Maintenance cost	Maintenance frequency (1/day) × maintenance factor (5%) × (capital cost per kg of product + catalyst cost + membrane cost)
Balance of plant	Balance of plant factor (35%) × (capital cost per kg of product + catalyst cost + membrane cost)
Operational cost	separation cost (20% of the of the total catalyst cost.) + other operational cost (10% of the electricity cost)
Electricity cost	operating voltage, FE%, and electricity price
Input chemical cost	Reactant 3-NS cost + electrolyte cost

Supplementary figures and tables

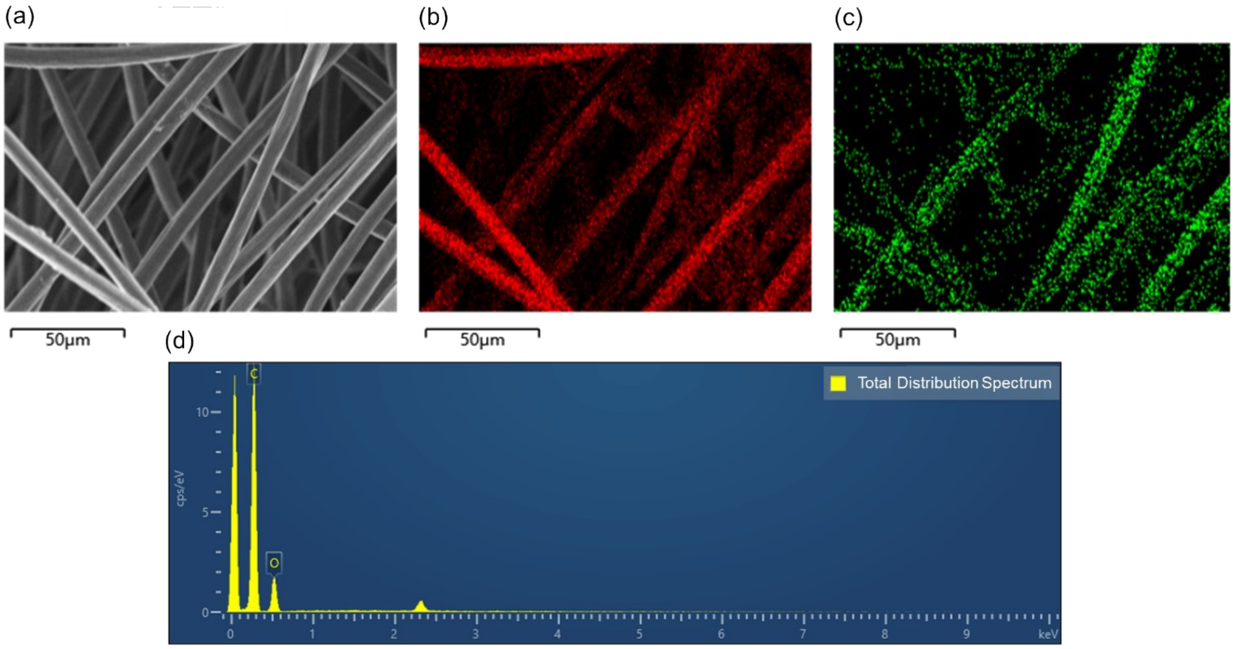

Figure S1. SEM characterization of OGF sample:(a) Macroscopic optical image;(b, c) EDS elemental mapping of C and O, respectively;(d) Corresponding total spectrum (C: 82.22 at%, O: 17.78 at%).

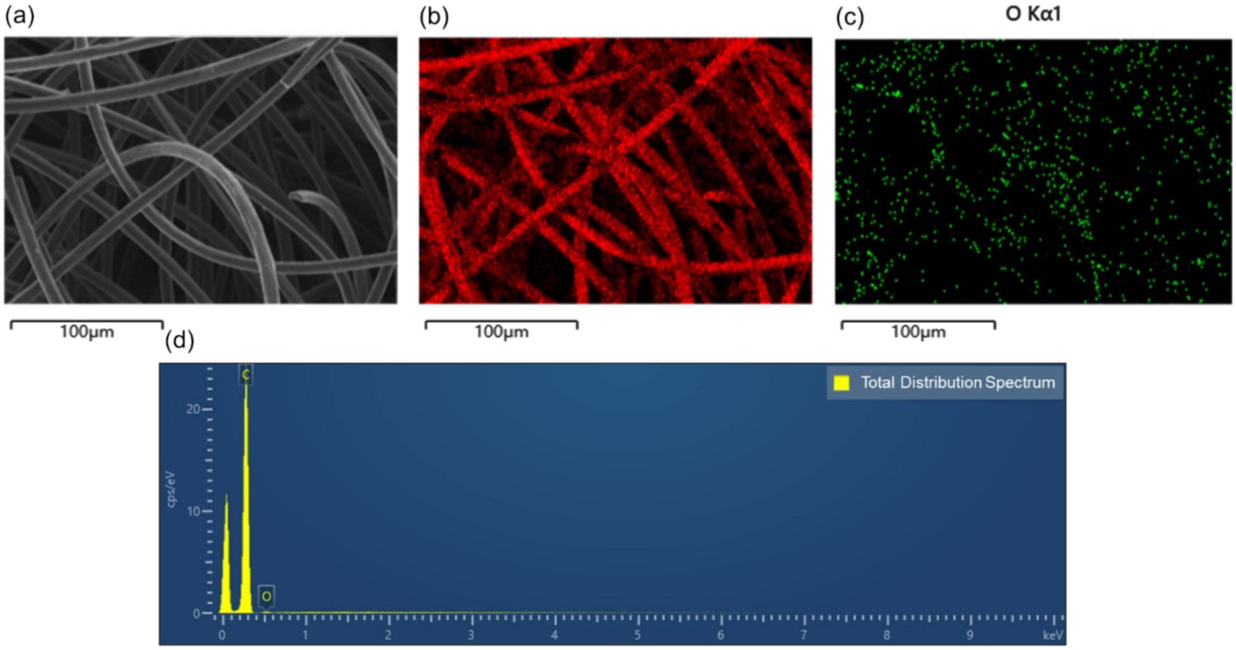

Figure S2. SEM characterization of RGF sample:(a) Macroscopic optical image;(b, c) EDS elemental mapping of C and O, respectively;(d) Corresponding total spectrum (C: 98.96 at%, O: 1.04 at%).

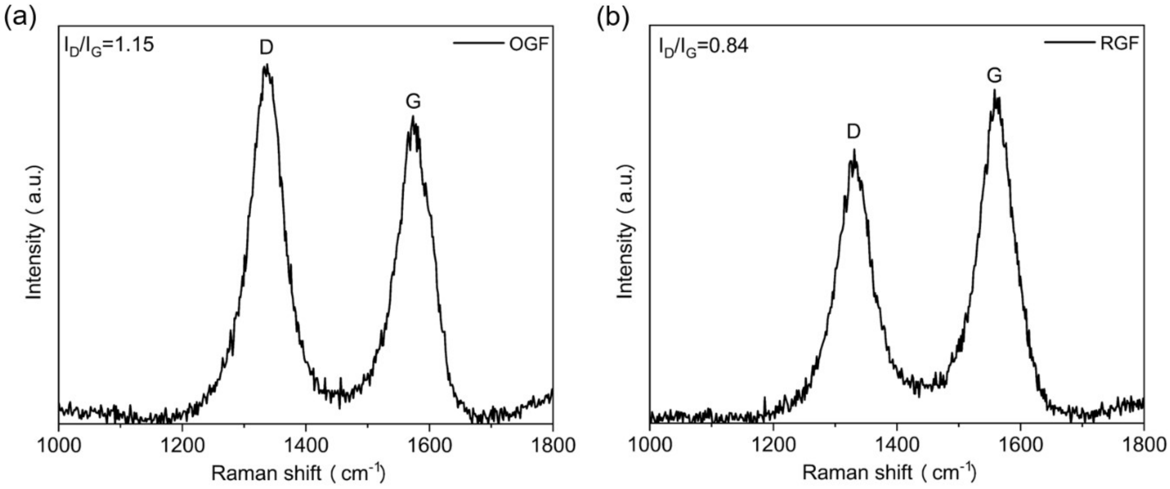

Figure S3. Raman spectra of OGF (a) and RGF (b)

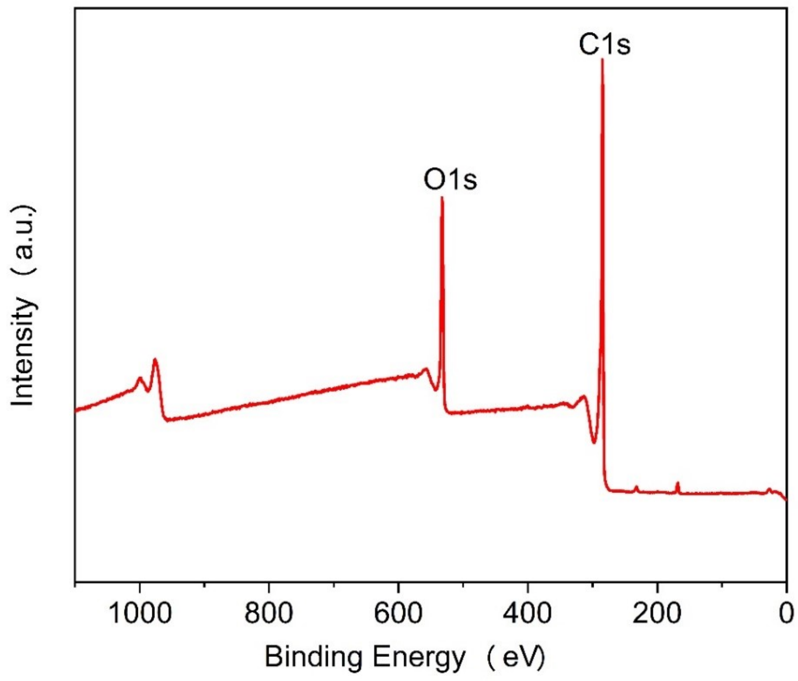

Figure S4. XPS survey spectrum of OGF

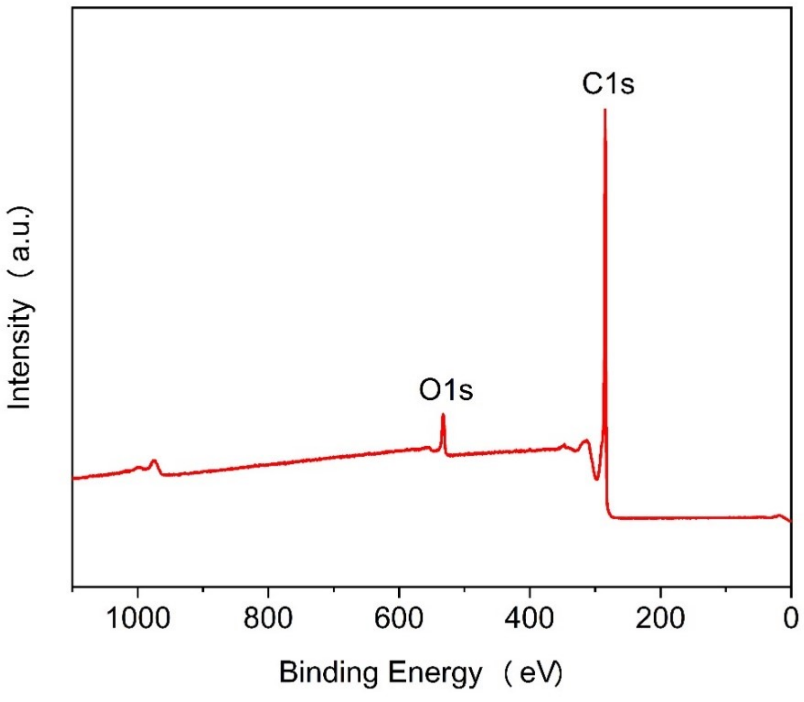

Figure S5. XPS survey spectrum of RGF

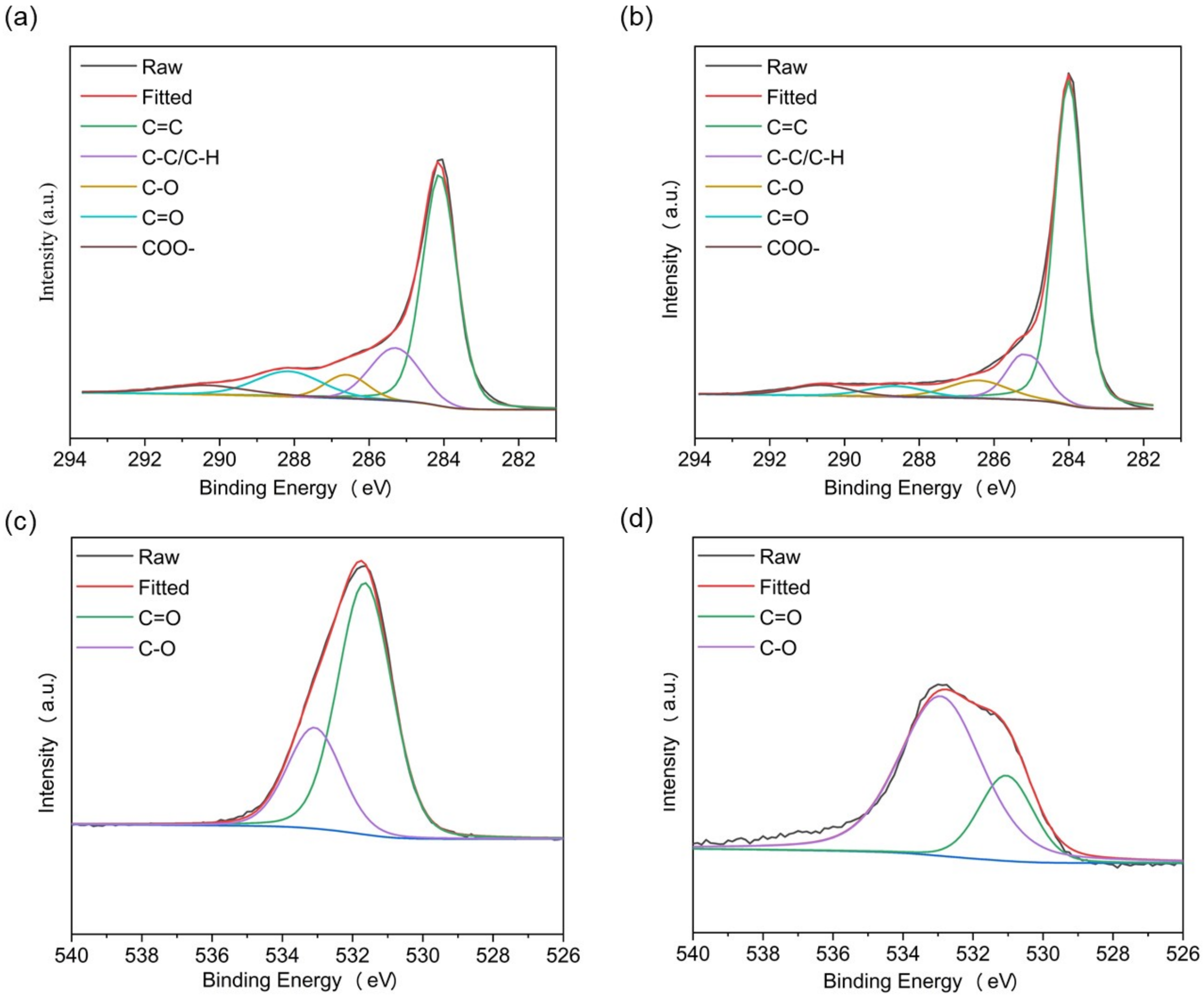

Figure S6. Comparison of C 1s (a, b) and O 1s (c, d) XPS spectra of OGF (a, c) and RGF (b, d). In the C 1s spectrum, the oxygen-containing peak of the OGF sample is significant; after treatment, the intensity of the oxygen-containing peak of the RGF sample decreases, and the carbon skeleton peak dominates. In the O 1s spectrum, the intensity of the C=O related oxygen peak of the OGF sample is significantly higher than that of the RGF sample; after treatment, the overall oxygen peak of the RGF sample decreases.

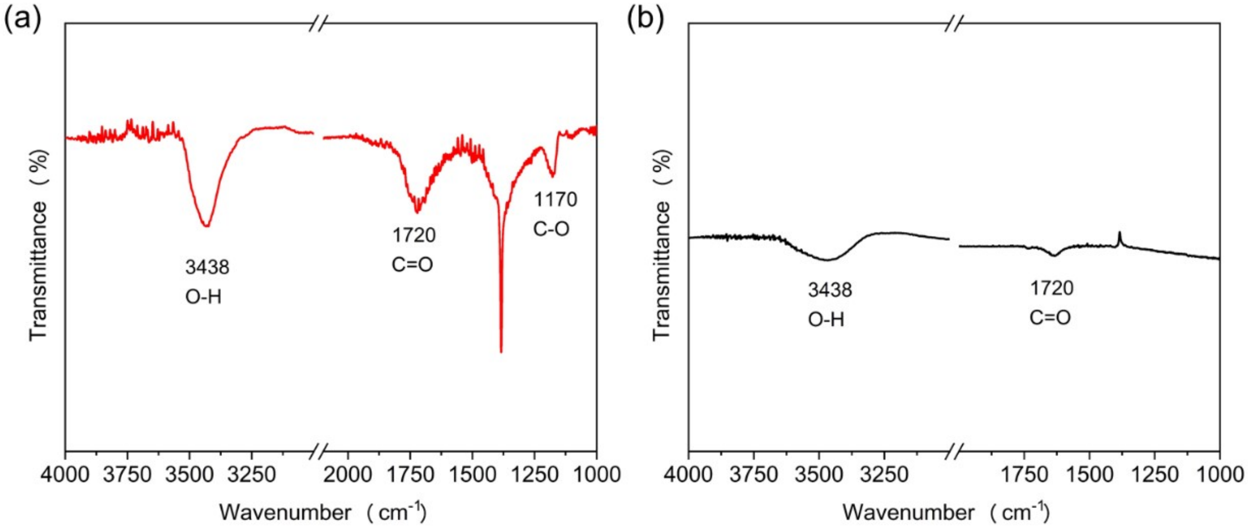

Figure S7. FT-IR of OGF (a) and RGF (b)

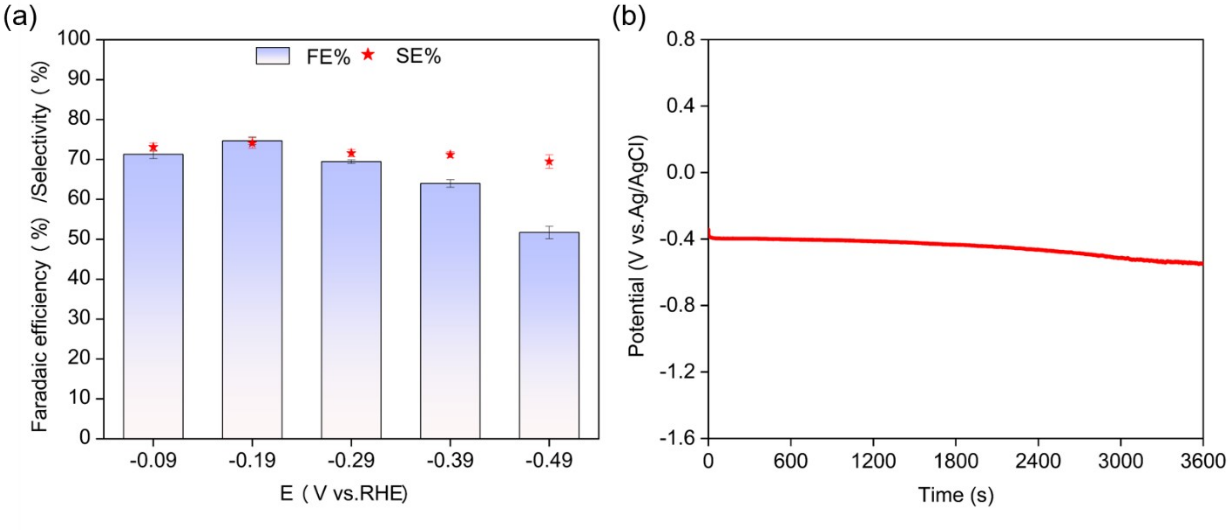

Figure S8. (a) The FE and selectivity of 3-VA at -0.09 to -0.49V vs. RHE (reaction time: 1h). Error bars correspond to the standard deviation of three independent measurements. (b) V-t curve for electrocatalytic reduction of 3-NSRR over OGF electrode (cathode) for 1 h at 30 mA·cm^{-2}.

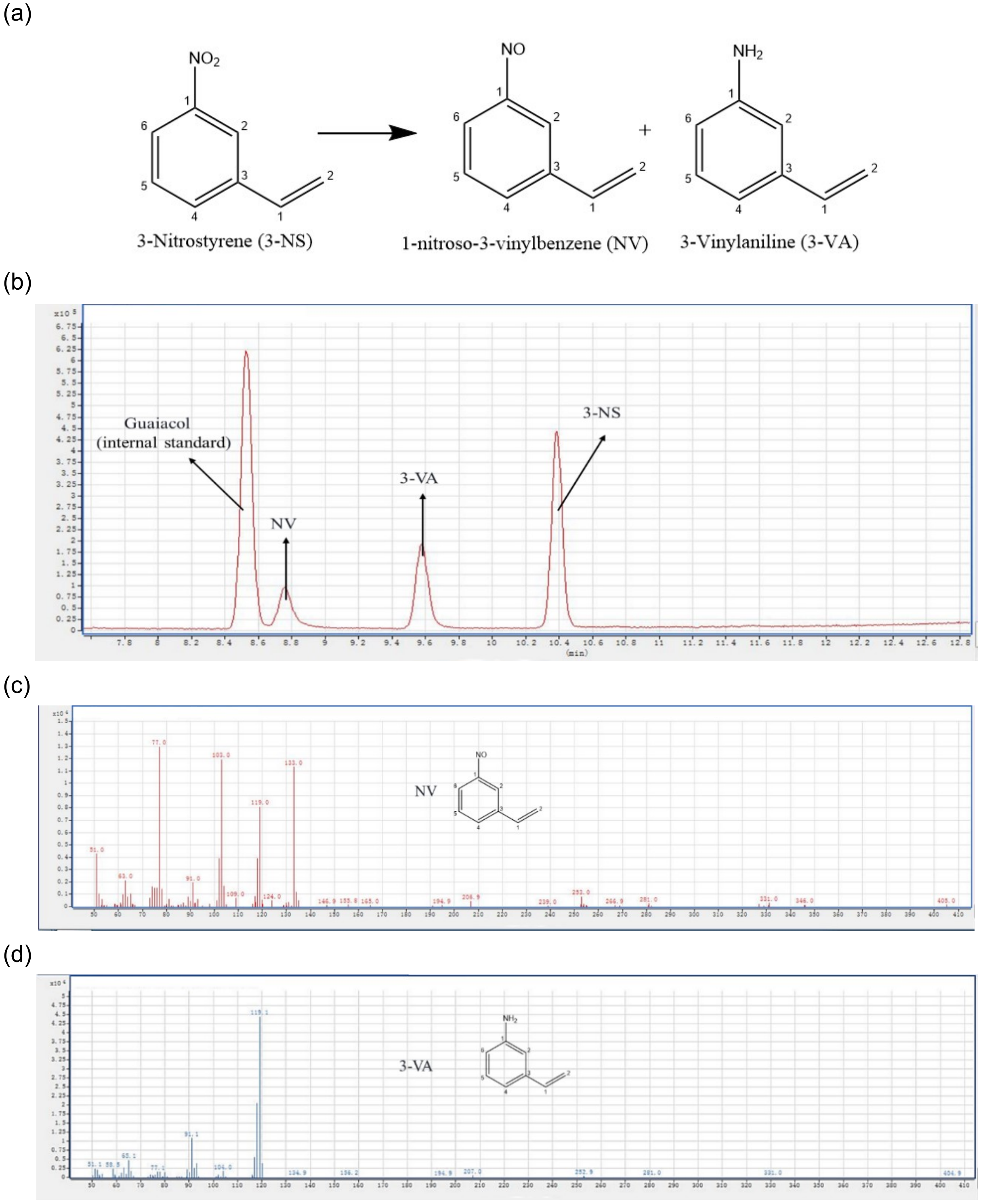
(a)
NO_2
3-Nitrostyrene (3-NS)
NO
1-nitroso-3-vinylbenzene (NV)
+
NH_2
3-Vinylaniline (3-VA)
(b)
x10 5
Guaiacol
(internal standard)
NV
3-VA
3-NS
(min)
(c)
x10 4
77.0
103.0
133.0
119.0
51.0
63.0
91.0
109.0
124.0
146.9
155.8
165.0
194.9
206.9
239.0
253.0
266.9
281.0
331.0
346.0
405.0
NV
NO
(d)
x10 4
119.1
3-VA
NH_2
91.1
51.1
55.5
65.1
77.1
104.0
134.9
156.2
194.9
207.0
252.9
281.0
331.0
404.9

(e)

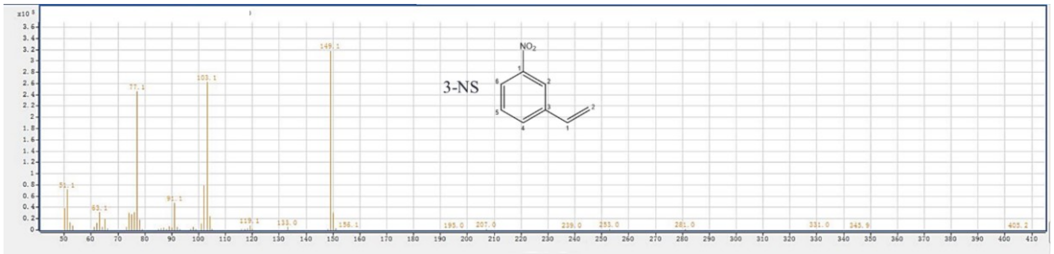

Figure S9. GC-MS results of products from electrocatalytic reduction of 3-NSRR on OGF catalyst and guaiacol **(**internal standard**)**. (a) electrocatalytic reduction of 3-NS to NV, and 3-VA. (b) GC-MS analysis. (c) Mass spectra from GC-MS analysis of NV. (d) Mass spectra from GC-MS analysis of 3-VA. (e) Mass spectra from GC-MS analysis of 3-NS.

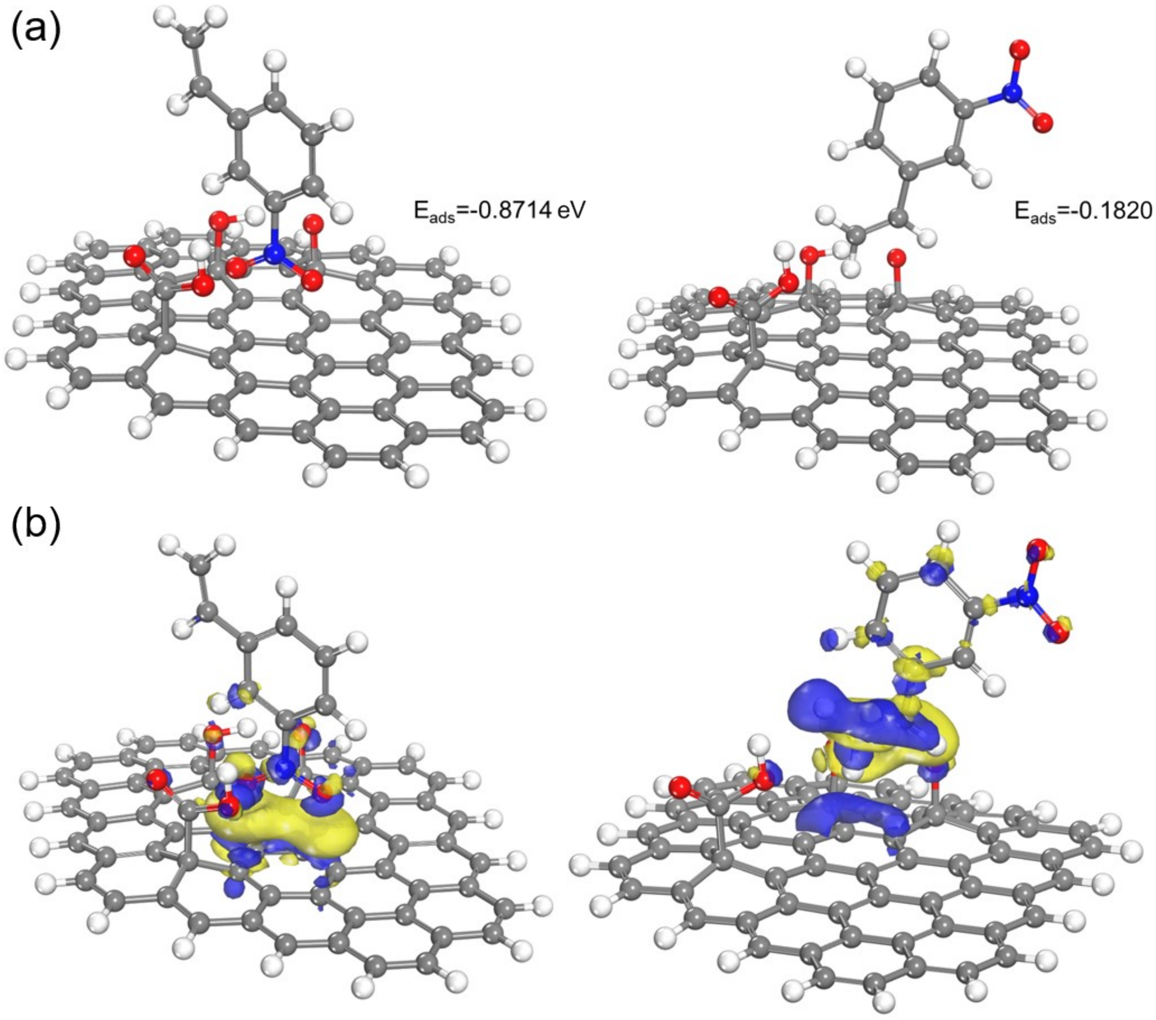

Figure S10. (a) Adsorption energy of the -NO_2 group (left) and C=C bond (right) on oxidized graphene edges via DFT calculation. (b) Corresponding charge density difference plots. The blue and yellow regions indicate electron accumulation and depletion, respectively. It can be observed that significantly more pronounced electron redistribution occurs at the catalyst-molecule interface in the -NO_2 group adsorption mode, thus confirming the stronger interaction between the nitro group and the catalyst surface at the electronic structure level.

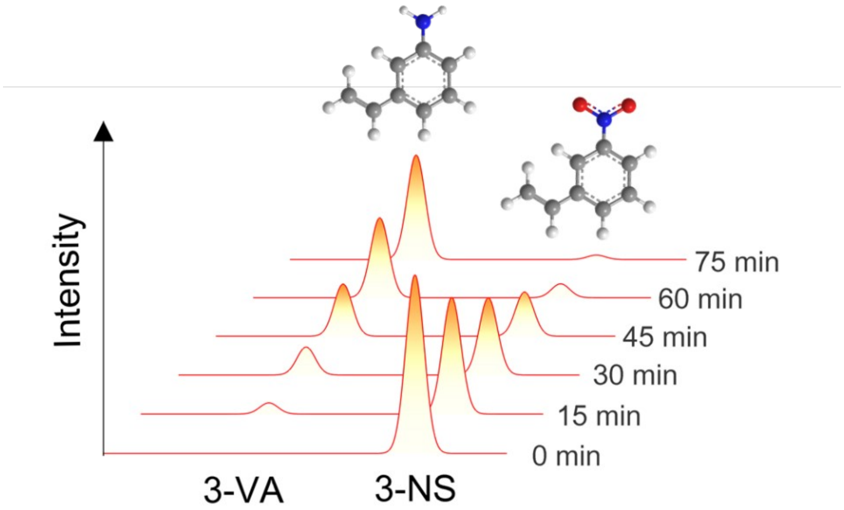

Figure S11. Concentration variation curves of the 3-NS and 3-VA over time.

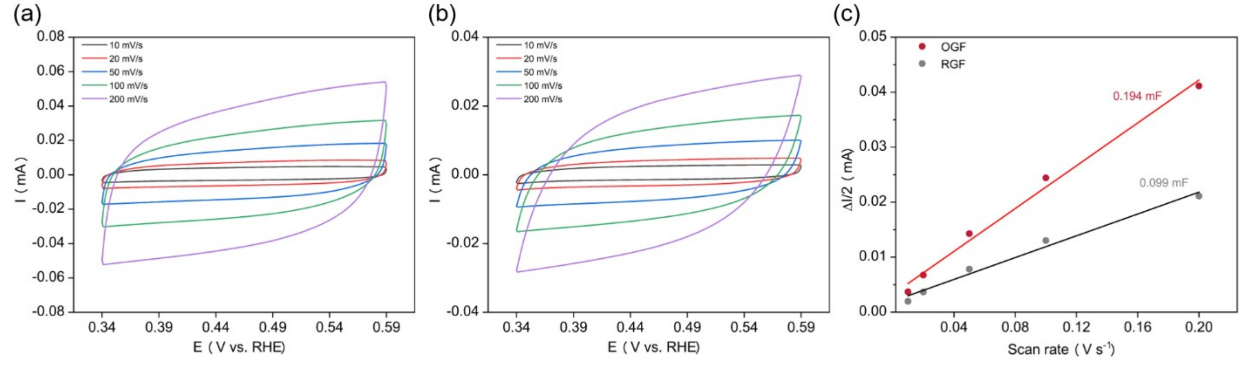

Figure S12. CVs of (a) OGF and (b) RGF in 0.16 M H_2SO_4. (c) Estimation of Cdl of OGF and RGF. Herein the specific capacitance a value of 20 μF cm^{-2} is adopted to calculate ECSA and make comparison.[12] The ECSA values of OGF and RGF were 9.7 and 4.95 cm^2, respectively.

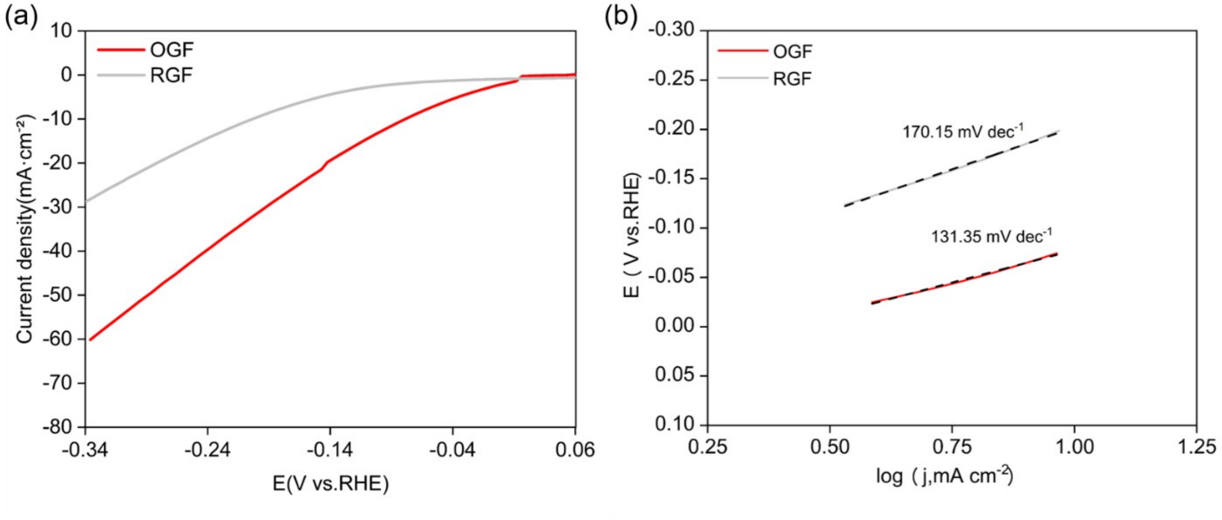

Figure S13. (a) LSV curves of the OGF and RGF electrodes in a solution containing 10mM 3-NS at a scan rate of 5mV s^{-1}. (b) Tafel plots corresponding to LSV.

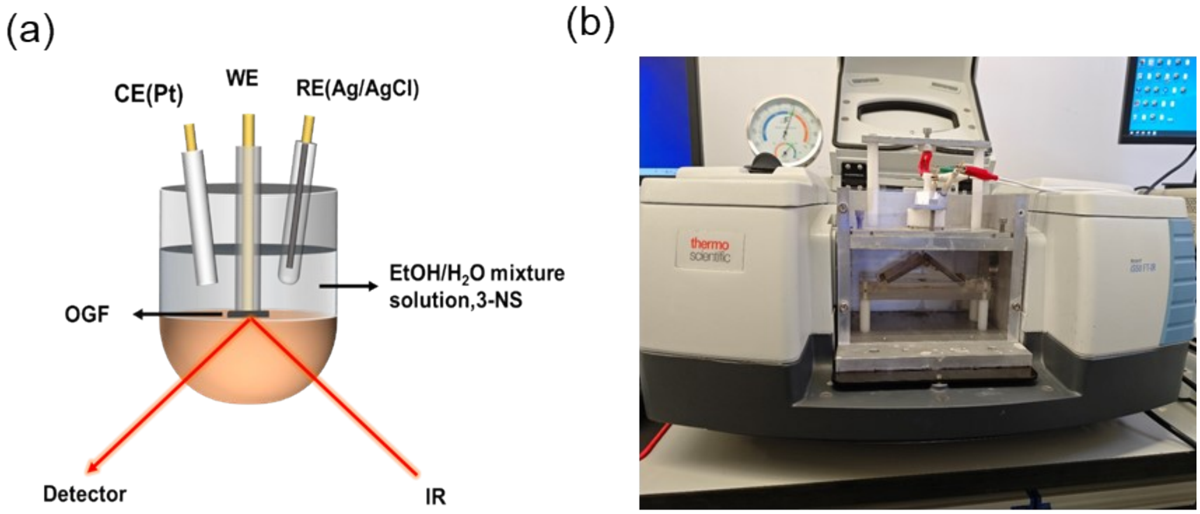

Figure S14. (a) In situ IRRAS configuration for the electrocatalytic reduction of 3-NSRR.OGF, Ag/AgCl, and Pt mesh as the work, reference, and counter electrode, respectively. (b)In-situ infrared reflection absorption spectroscopy (IRRAS, Thermo Scientific Nicolet iS50 FT-IR), equipped with an A-type mercuric cadmium telluride (MCT) detector.

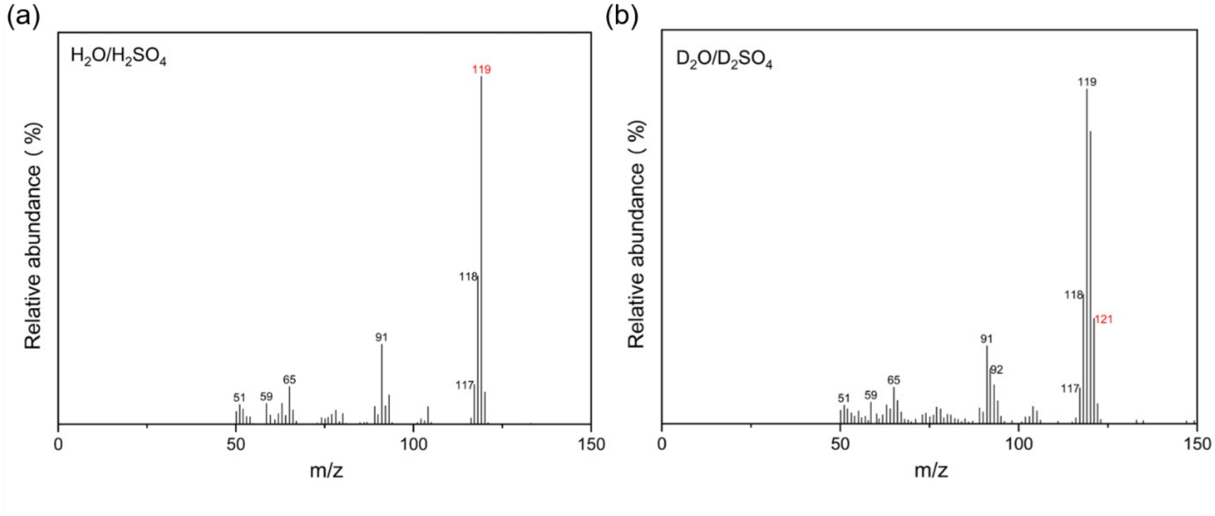

Figure S15. Mass spectra of 3-VA obtained with H_2O/H_2SO_4 (a) or D_2O/D_2SO_4 (b) as the electrolyte of the electrocatalytic reduction of 3-NS.

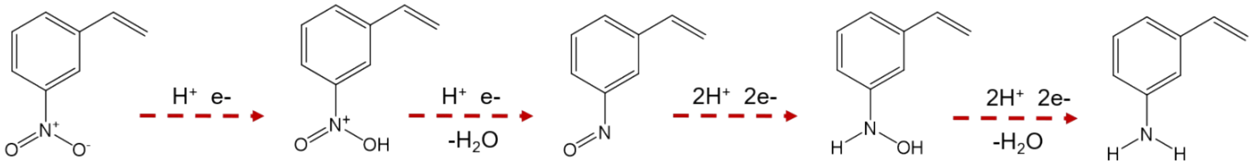

Figure S16. Proposed mechanism of highly selective electrochemical reduction of 3-nitrostyrene over OGF cathode in 0.16 M H_2SO_4 solution.

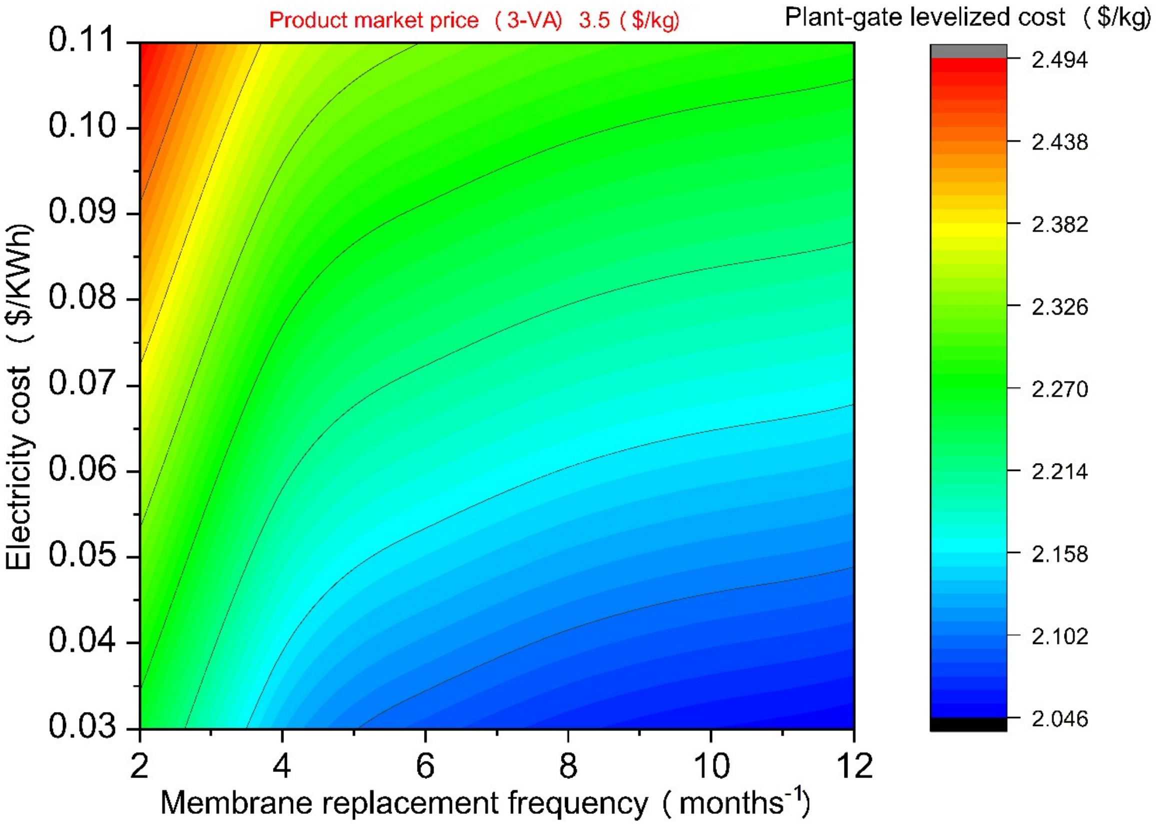

Figure S17. Sensitivity analysis of the levelized production cost for 3-VA. This contour plot illustrates the combined effects of electricity cost (y-axis) and membrane replacement frequency (x-axis) on the plant-gate levelized cost ($/kg, represented by contour lines). The analysis is based on a baseline production capacity of 1000 kg per day. The results identify a broad operational window within which the electrochemical process remains economically competitive.

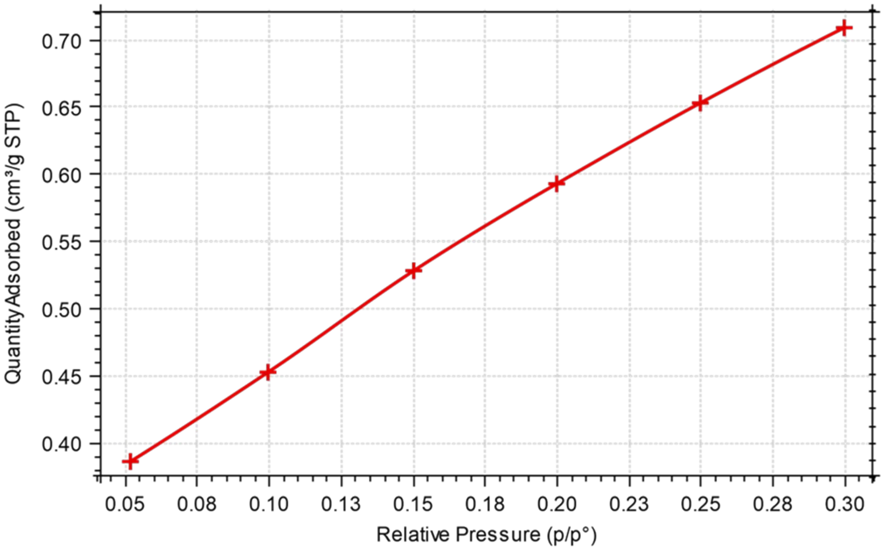

Figure S18. The N_2 adsorption isotherm. The BET surface area of the OGF was measured to be 2.3059 m^2/g, indicating enough active sites for nitro groups reduction.

References

1. W. Zhang, W. Zhang, K. Yu, J. Tan, Y. Tang and Q. Gao, *Chem. Sci.*, 2024, **15**, 3446-3452.
2. W. Zhang, W. Zhang, J. Tan, D. Pan, Y. Tang and Q. Gao, *J. Mater. Chem. A*, 2023, **11**, 7505-7512.
3. Y. Zhao, C. Liu, C. Wang, X. Chong and B. Zhang, *CCS Chem.*, 2020, **3**, 507-515.
4. X. Chong, C. Liu, Y. Huang, C. Huang and B. Zhang, *Natl. Sci. Rev.*, 2020, **7**, 285-295.
5. J. Tan, J. Shao, Y. Shi, W. Zhang and Q. Gao, *ACS Sustainable Chem. Eng.*, 2022, **10**, 13525-13533.
6. H. An, Y. Ding, P. Sautet, G. Sun and N. Yan, *J. Am. Chem. Soc.*, 2024, **146**, 29315-29324.
7. T. Peng, T. Zhuang, Y. Yan, J. Qian, G. R. Dick, J. Behaghel de Bueren, S.-F. Hung, Y. Zhang, Z. Wang, J. Wicks, F. P. Garcia de Arquer, J. Abed, N. Wang, A. Sedighian Rasouli, G. Lee, M. Wang, D. He, Z. Wang, Z. Liang, L. Song, X. Wang, B. Chen, A. Ozden, Y. Lum, W. R. Leow, M. Luo, D. M. Meira, A. H. Ip, J. S. Luterbacher, W. Zhao and E. H. Sargent, *J. Am. Chem. Soc.*, 2021, **143**, 17226-17235.
8. T. Peng, W. Zhang, B. Liang, G. Lian, Y. Zhang and W. Zhao, *Nat. Commun.*, 2023, **14**, 7229.
9. P. De Luna, C. Hahn, D. Higgins, S. A. Jaffer, T. F. Jaramillo and E. H. Sargent, *Science*, 2019, **364**, eaav3506.
10. W. R. Leow, Y. Lum, A. Ozden, Y. Wang, D.-H. Nam, B. Chen, J. Wicks, T.-T. Zhuang, F. Li, D. Sinton and E. H. Sargent, *Science*, 2020, **368**, 1228-1233.
11. M. Jouny, W. Luc and F. Jiao, *Ind. Eng. Chem. Res.*, 2018, **57**, 2165-2177.
12. M. A. Ashraf, S. Daskalakis, M. Kogler, M. Ostermann, S. Gahlawat, S. Son, P. Mardilovich, M. Valtiner and C. M. Pichler, *Nanoscale*, 2024, **16**, 7926-7936.